Journal of Nuclear Materials 405 (2010) 109–117

Contents lists available at ScienceDirect

Journal of Nuclear Materials

journal homepage: www.elsevier.com/locate/jnucmat

Changes to the reflectance of Be mirrors due to deuterium plasmas contaminated with oxygen

A.F. Bardamid [a], V.N. Bondarenko [b], J.W. Davis [c,*], V.G. Konovalov [b], O. Litvin [d], I.V. Ryzhkov [b], A.N. Shapoval [b], A.F. Shtan' [b], S.I. Solodovchenko [b], V.S. Voitsenya [b]

[a] Taras Shevchenko National University, 01033 Kiev, Ukraine
[b] IPP NSC KIPT, 61108 Kharkov, Ukraine
[c] University of Toronto Institute for Aerospace Studies, 4925 Dufferin St., Toronto, ON, Canada M3H5T6
[d] Institute of Semiconductor Physics of NASU, 41, pr. Nauki, Kiev 03028, Ukraine

ARTICLE INFO

Article history:
Received 8 February 2010
Accepted 26 July 2010

ABSTRACT

The reflectance of Be mirrors due to impact by ions from a deuterium plasma has been studied under several bombardment conditions. Analysis of the resulting surface films has been performed using various diagnostic techniques, with the conclusion that the primary factor leading to the decrease in reflectance following bombardment with energetic ions is the conversion of the surface oxide layer, composed of BeO, to the hydroxide, $Be(OD)_2$, with a corresponding increase in the optical extinction coefficient. The increase in the thickness of the layer is also important. Modifications to the surface layer are thought to involve a balance between the ion-induced diffusion of Be atoms to the surface where they may react with incident D and O atoms, and physical and chemical sputtering processes. For incident ion energies less than ~50 eV, chemical reactions leading to disoxidation of the oxide–hydroxide film dominate, while keV-range ions (primarily D, but with some O impurities) lead to the formation of hydroxide, and an increase in the surface layer thickness.

1. Introduction

The current baseline design for ITER specifies that first wall armor tiles will be made of beryllium. Experience with current fusion devices thus suggests that beryllium will be the primary element deposited on remote inner surfaces. In particular, the mirrors of some optical and laser diagnostics, necessarily located in positions line of sight to the plasma, may quickly become coated by a layer of beryllium. Since a Be film as thin as 20 nm would convert the reflectance of a mirror of any other material to a reflectance close to that of beryllium, it may make more sense to begin operation in ITER with solid Be mirrors. This reasoning has led to the investigation of the behavior of Be mirrors exposed to deuterium plasmas, with some results published in previous papers [1–3].

However, recent Be deposition experiments on PISCES-B [4] have shown that the Be films deposited on W or Cu mirror specimens had a very high porosity and their reflectance was much lower than the reflectance of bulk Be mirrors. While this does not rule out the use of solid Be mirrors, it highlights the need for further experiments to aid in the understanding of beryllium surfaces exposed to hydrogen plasmas.

In this paper, we review the latest results on experiments with Be mirrors with the following intentions: (i) the properties of deposited films strongly depend on the deposition conditions, and it is possible that the reflectance of the Be film deposited on some in-vessel mirrors would be similar to the reflectance of a bulk Be mirror; (ii) new results are available which help to explain the changes to the optical properties of Be mirrors observed in [1–3] as being the result of surface chemistry involving oxygen impurities in the deuterium plasma; (iii) since beryllium is being used, or is planned for mirrors on space-based telescopes (e.g. [5,6]), the chemical processes on the surface of Be mirrors subjected to mixtures of hydrogen and oxygen ions may also simulate the experience of Be mirrors on such satellites.

During the experiments on Be mirrors described in [1–3], a complex reflectance behavior during exposure to deuterium plasmas ions was observed: there was a sharp drop of reflectance after short exposures to keV-energy ions, followed by the near full restoration of the reflectance when the mirrors were subsequently exposed to low-energy (~50 eV) ions from the same plasma. It was hypothesized in [3] that such behavior is caused by some chemical processes on the mirror surface. Recent work with Al mirrors [7], as well as further experiments with Be, have related the changes in reflectance to changes in the thickness and composition of the surface oxide layer. The experiments with Al mirrors were prompted by the diagonal analogy between Be and Al [8], and because of the

* Corresponding author at: University of Toronto Institute for Aerospace Studies, 4925 Dufferin St., Toronto, ON, Canada M3H5T6.
E-mail address: jwdavis@starfire.utias.utoronto.ca (J.W. Davis).

0022-3115/$ - see front matter © 2010 Elsevier B.V. All rights reserved.
doi:10.1016/j.jnucmat.2010.07.039

wider range of surface diagnostics available for Al (due to safety considerations). It was found that Al mirrors have a very similar reflectance behavior to Be [7], and surface analysis by Auger electron spectroscopy and secondary ion mass spectrometry (SIMS) have given additional support to the proposed surface processes (in Section 4 we also show some results from experiments with Al mirrors).

The increase in thickness of the oxidized layer on a Be surface due to radiation induced oxidation was first observed [9] during exposure of Be specimen to bombardment with D^+ and He^+ ions of 2.5 and 5 keV, respectively, under vacuum conditions, but with a partial pressure of oxygen-containing molecules of 10^{-5} Pa. Much later the authors of [10] observed the increase of an oxidized surface film when a Be specimen was exposed to deuterium atoms. Based on the composition of the SIMS spectrum, the authors of [10] came to the conclusion that the increase in film thickness is mainly due to formation of beryllium hydroxide, $Be(OD)_2$ according to reaction: $2BeO + 2D \Rightarrow Be(OD)_2 + Be + 0.7$ eV/D.

The present paper builds on these results, further developing the mechanisms involved in the formation and transformation of the surface oxide layers, and the effect on reflectance.

2. Experimental

The mirror specimens, disks 30 mm in diameter and 3 mm thick, were fabricated of hot pressed beryllium with different grain sizes. Two further specimens of dimensions $13 \times 13 \times 8$ mm were analyzed by X-ray photo-electron spectroscopy (XPS) to give the chemical composition of the surface oxide layers following exposure to the deuterium plasma. Specimens were exposed to ions extracted from a deuterium plasma in a device (DSM-2) with a double-mirror magnetic configuration operated at the electron cyclotron resonance conditions (magnetron frequency 2.37 GHz) [11,12]. The base pressure in the vacuum system was $\sim 2 \times 10^{-4}$ Pa, while during operation, the deuterium pressure was around 2×10^{-2} Pa. With a magnetron power of ~400 W, the plasma parameters were: $n_e \approx 10^{16}$ m^{-3}, $T_e \sim 5$ eV. The copper specimen holder was water-cooled and placed on the system axis, just outside the magnetic mirror; it was biased negatively at a fixed potential in the range 30–2000 V.

After every exposure event the reflectance of the mirror specimens was measured *ex situ* at normal incidence in the range 220–650 nm. Also, for a couple of Be samples *in situ* measurements of reflectance at a wavelength 650 nm were made as a function of the exposure time. Ellipsometry was used to find the optical indices, and an additional characterization of the optical properties, namely, the ability of a mirror to transmit the image of a luminous object (image quality, IQ), was measured at a special stand.

3. Experimental results

3.1. Dependence of reflectance on ion energy

We have previously published similar measurements [2,3] but with low statistics and a limited set of Be mirror specimens. Thus, the experiments were repeated with Be specimens with different structures and purities. Two identical Be mirror samples (TGP-56, BeO content 0.9–1.3%, grain size 50–60 μm) were repeatedly exposed, in turn, to ions of different energies in the range 30–2000 eV and after each exposure the behavior of their reflectance was measured *ex situ* using a 2-channel scheme as in [11,12]. Every time the ion energy exceeded ~60 eV a decrease of the specular reflectance was observed, with the magnitude of the decrease increasing with increasing ion energy. This is shown in Fig. 1 for two wavelengths, indicated by "down" in the legend. Note that

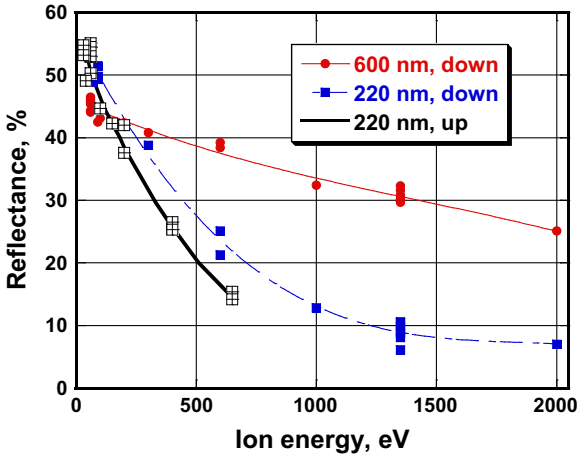

Fig. 1. Ion energy dependences of the drop (curves "down") and restoration (curve "up") of reflectance for two Be samples.

some points of these graphs were obtained with mixture of deuterium and helium with estimated ratios (35–40)/(65–60) of partial pressure of deuterium (the sum of masses 3 and 4) to helium pressure. The use of He in the plasma will be discussed below.

It was found that the decrease in reflectance can be partly restored by exposing the mirror not only to low-energy ions of ~50 eV, as was found earlier [2,3], but to ions with any energy below that of the initial bombardment. However, to have a full restoration of reflectance, the exposure to lower energy ions has to last for a much longer time (about an order of magnitude) than the initial bombardment with the more energetic ions which led to the drop of reflectance. This ion energy dependence of restored values of reflectance at $\lambda = 220$ nm is shown as the curve "up" in Fig. 1. It is seen that the higher energy of ions used during the restoration procedure, the lower the degree of reflectance restoration in comparison with its initial level. A full recovery of reflectance took place only for ion energies below 60 eV. A careful analysis of the low-energy range (0–200 eV) found that a full restoration of reflectance, as measured at $\lambda = 220$ nm, can be reached for ion energies ~30–40 eV, while the threshold for the drop in reflectance is near 55–65 eV; an experimental accuracy of 1–1.5% on the reflectivity measurements limits the further narrowing these energy intervals.

In comparing the data obtained with deuterium and deuterium–helium plasmas, some quantitative differences in behavior was observed, see Fig. 2. The D_2 + He plasma exposure resulted in a somewhat larger decrease in reflectance as compared to the case of D_2 plasma. This will be discussed later.

An important result obtained during these experiments is that the two Be mirror specimens passed through many drop-restoration procedures and the total ion fluence amounted to $\sim 2.5 \times 10^{26}$ ion/m^2 (the total exposure time exceeded 60 h for each mirror, with a mean ion current density ~15 A/m^2). However, they continued to exhibit a high ability to transmit an image (high IQ), as demonstrated in Fig. 3: the IQ profiles of an Al etalon and a Be mirror were found to have an ideal coincidence [13]. This fact is additional evidence that the reflectance changes are not connected with modifications to the Be metal surface (i.e., development of the microrelief) but are due to chemical processes in the surface oxide layers, as postulated in [1–3].

3.2. Ellipsometer measurements

The degradation of Be mirror reflectance due to bombardment with keV-energy range ions in the DSM-2 device is thought to be caused by the transformation of the surface oxide layer partially into a hydroxide [3]. To find the optical properties of the

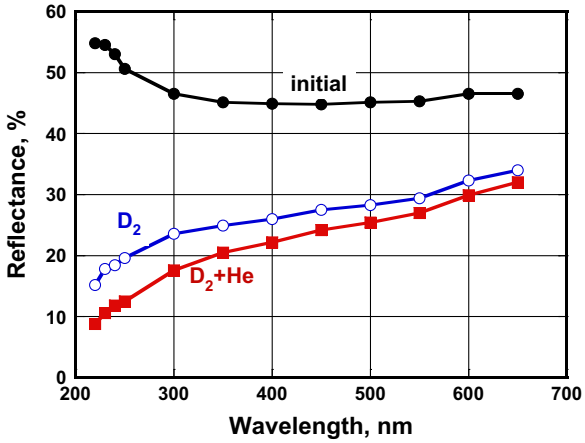

Fig. 2. Wavelength dependences of the initial reflectance (after cleaning with 60 eV ions) and the reflectance following subsequent exposure to similar fluences of ions of deuterium or deuterium–helium plasmas with energies of 1.35 keV.

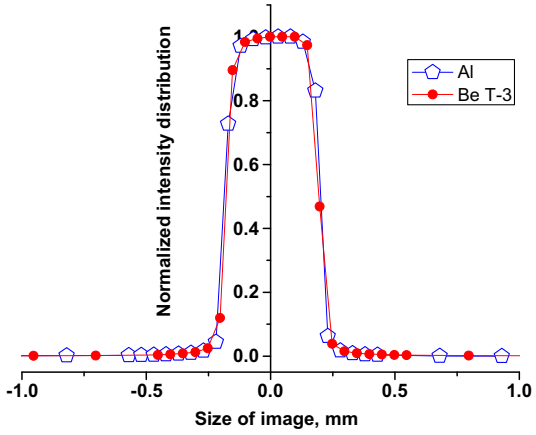

Fig. 3. Normalized IQ profiles for an Al etalon and for one of two beryllium mirror specimens following the numerous plasma-ion exposures resulting in data shown in Fig. 1.

transformed film and to estimate its thickness, the ellipsometry method was used. In this section, we describe the main results obtained by ellipsometry; to distinguish between the initial state of mirror surface and the transformed state we will use the terms 'oxide' and 'hydroxide' films, respectively.

The above results of reflectance at normal incidence, $R(\lambda)$, in the range $\lambda = 220$–650 nm were obtained by *ex situ* measurements after every exposure of specimens to some ion fluence. Spectral reflectance could also be evaluated from the spectral polarization angles $\Psi_m(\lambda)$ and $\Delta_m(\lambda)$ obtained by means of a spectral ellipsometer ($\lambda = 380$–720 nm, angle of incidence 50° or 75°) with a rotating analyzer (RAE). Using the data on polarization angles, the spectral optical indices (refraction, n, and extinction, k) of the film and the film thickness were found. The evaluation of spectral optical indices was also made at one wavelength by the multiangular method using a standard laser ellipsometer (LEF-3M-1, $\lambda = 632.8$ nm, angle of incidence 45–80°). The data obtained from both ellipsometers were processed in a model consisting of a homogeneous single-layer film on the surface of a Be substrate.

Using the data on the polarization angles $\Psi_m(\lambda)$ and $\Delta_m(\lambda)$, the spectral optical constants of the oxide or hydroxide layer (refraction index $n(\lambda)$ and extinction coefficient $k(\lambda)$), and the film thickness d were calculated for two Be mirror specimens, Be4B and Be4H, that had initially very similar optical characteristics. For calculation of reflectance for Be specimens without a surface film (clean surface model) and with an isotropic homogeneous film in the single-layer-film model (oxide or hydroxide), the optical indices $n_0(\lambda)$, $k_0(\lambda)$ of pure beryllium [14] were adopted.

The optical indices $n_1(\lambda)$, $k_1(\lambda)$ of the surface oxide are shown in Fig. 4 for specimen Be4B after exposure to deuterium ions of $E_i = 60$ eV (ion current density $j = 14.7$ A/m^2, duration $\Delta t = 90$ min), and specimen Be4H after exposure to Ar ions ($E_i = 300$ eV, $j = 8.5$ A/m^2, $\Delta t = 10$ min). The calculated thickness of the oxide films on both specimens is about equal: $d_{4B} \approx d_{4H} \approx 8$ nm. At the wavelength λ_{He-Ne} the optical indices of the oxide are $n_1 = 1.62$, $k_1 = 0$ for Be4B and $n_1 = 1.77$, $k_1 = 0.03$ for Be4H. The calculated spectral reflectance of both specimens with oxide films, together with measured reflectance values are shown in Fig. 5 (oxide label). Also shown is the calculated spectral reflectance for a clean Be mirror.

The agreement between the calculated spectral reflectance and the measured ones confirms the correctness of the choice of models used in the ellipsometric evaluation. Within the range $\lambda = 380$–650 nm the best agreement between calculated reflectance $R_{ce}(\lambda)$ with measured $R_m(\lambda)$ was found for specimen Be4H with a surface

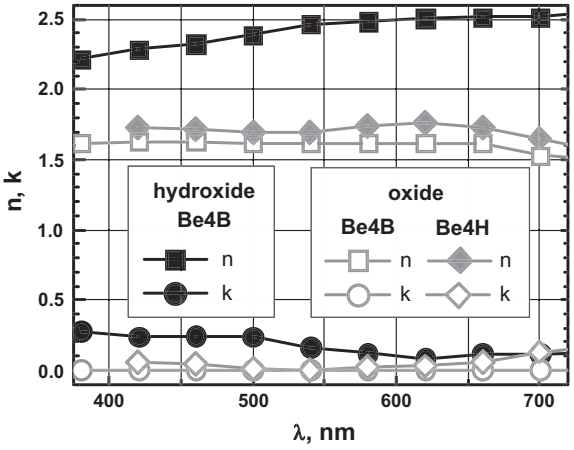

Fig. 4. The spectral indices of an oxide film on specimens Be4B, Be4H after cleaning with low-energy ions, from a D or Ar plasma, respectively. Also shown are the indices of a hydroxide film on specimen Be4B after bombardment with high energy ions from a D plasma.

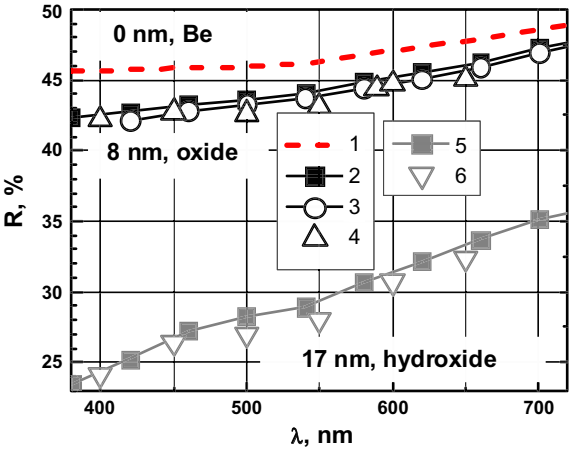

Fig. 5. The calculated reflectance of: 1 – Be mirror using a clean surface model, 2 – Be4B with oxide, 3 – Be4H with oxide, 5 – Be4B with hydroxide. Also shown are the measured reflectance of: 4 – Be4H with oxide, 6 – Be4B with hydroxide. The calculated thickness is indicated near the corresponding curve.

oxide layer: $|R_{ce}(\lambda) - R_m(\lambda)| < 1\%$. Thus, the basic spectral indices for an oxide film on Be were taken from the Be4H results.

In Fig. 4 the indices of the hydroxide film on sample Be4B formed after bombardment with high energy deuterium plasma ions ($E_i = 1.35$ keV, $j = 21.4$ A/m^2, $\Delta t = 21$ min) are also shown (hydroxide label). The thickness of the film has increased to ~17 nm. The indices are: $n_2 = 2.22$, $k_2 = 0.28$ at $\lambda = 380$ nm and $n_2 = 2.5$, $k_2 = 0.08$ at $\lambda = 650$ nm. The calculated spectral reflectance, $R_{ce}(\lambda)$, for the Be4B specimen with hydroxide film is very close to the measured one, $R_m(\lambda)$: $|R_{ce}(\lambda) - R_m(\lambda)| \lesssim 1.5\%$, as is shown in Fig. 5 (labels 5 and 6).

In analyzing the ellipsometry data for the Be specimens, it is seen that both the D and Ar plasma cleanings are rather effective, giving similar effects on spectral indices, film thickness (Fig. 4) and reflectance (Fig. 5) for specimens Be4B and Be4H. The principal difference is that for acceptable cleaning the exposure times must be much longer for the low-energy deuterium ions, than for the more energetic Ar ions. This is due to the different cleaning mechanism, chemical erosion and physical sputtering for D and Ar, respectively. However, with Ar ions some precautions have to be taken, as there is a possibility of developing roughness on the surface through extensive sputtering.

The oxide film indices in Fig. 4 ($n_1 = 1.51$–1.76, $k_1 \approx 0$) tend toward data for pure BeO films deposited on a sapphire plate, $n_1(\lambda) = 1.67$–1.65, $k_1(\lambda) = 0$ [15]. The spectral indices of the hydroxide film ($n_2 = 2.22$–2.51, $k_2 = 0.08$–0.28) are noticeably higher than the oxide film values ($n_1 = 1.68$–1.78, $k_1 \approx 0$) within the wavelength range $\lambda = 380$–650 nm. Thus, the oxide film on Be specimens is almost transparent and significantly thinner ($d = 8$ nm) than the hydroxide film; the latter is thicker ($d = 17$ nm) and has a non-zero extinction coefficient. Thus, the chemical change from an oxide layer to a hydroxide layer fully explains the drop of reflectance observed following exposure of Be mirrors to the keV-energy range ions from the deuterium plasma.

3.3. Composition of the surface layer

Measurements of the chemical composition of the surface layers for one of the square Be specimens was made by sputter-XPS at different points in the plasma-exposure cycles. The reflectance behavior of this specimen at two wavelengths is shown in Fig. 6 as a function of the total fluence of deuterium plasma ions. As indicated on the figure, the consecutive exposures to keV-energy ions (procedure 1) and to low-energy ions (procedure 2) were repeated for this particular sample 4 and 3 times, respectively, with a full restoration of reflectance after every long-term exposure to 60 eV ions.

The XPS analyses were made three times, indicated by marks X1, X2, X3 on Fig. 6: after cleaning by 10 min exposure to 300 eV Ar^+ ions (position X1), after a 35 min exposure to ions from a deuterium plasma with 1350 eV incident energy (position X2), and after the second recovery procedure, 4.3 h exposure to low-energy (60 eV) ions (position X3). The results of XPS measurements are shown in Fig. 7.

The results of the XPS analysis are consistent with ellipsometry measurements, with the keV-ion bombardment leading to a thicker oxygen-containing surface layer, and the low-energy ion bombardment leading to a thinner surface layer. Unfortunately, the small energy shift between the bonding lines corresponding to beryllium oxide and beryllium hydroxide prevented information about the hydroxide character of the surface from being determined. The mechanisms involved in these transformations will be discussed later.

3.4. Exposure time dependence of reflectance

The addition of *in situ* optical techniques has enabled more detailed measurements of the time dependence of the reflectance changes at one wavelength (650 nm), Fig. 8. It was found that a significant drop of the reflectance, $\Delta R(t) = R(t) - R_0$, occurs after only 1 min of ion exposure, see Fig. 9: curves with open squares and open circles of Fig. 9 are for parts 1–2 and 3–4 of the reflectance time dependence in Fig. 8, respectively. One minute is the minimum time required for stable discharges to be established in DSM-2, and the 1 min ion fluence corresponds to $\sim 7 \times 10^{21}$ ion/m^2. A comparison with *ex situ* measurements at 650 nm is also shown on Fig. 9 (solid squares). The qualitative agreement between the *in situ* and *ex situ* measurements of the reflectance is clearly seen, though the *ex situ* data appear to demonstrate a saturation of the reflectance drop behavior sooner than the *in situ* data. This qualitative agreement confirms that a relatively short (few hours) exposure to air prior to the *ex situ* measurements does not have significant influence on the optical properties. Further, the full restoration of reflectance (parts 2–3 of the curve in Fig. 8) again is an indication that the change in reflectance is connected with chemical processes on the surface and not with the appearance of roughness.

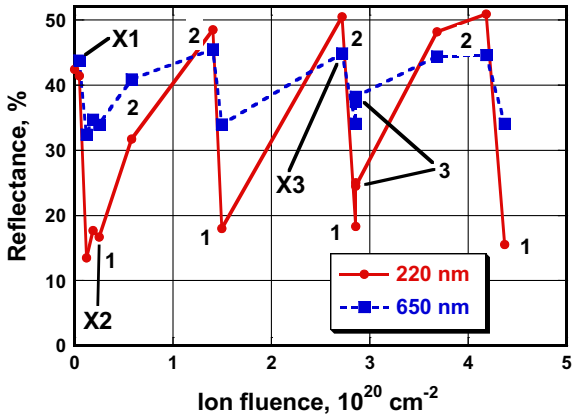

Fig. 6. Total ion fluence dependence of reflectance at the indicated wavelengths for Be mirror specimen prepared for XPS analysis. 1 – Indicates the drops of reflectance due to bombardment with 1350 eV ions, 2 – restoration of reflectance due to bombardment with 60 eV ions, 3 – vacuum annealing (2 h at 200 °C) after the drop of reflectance.

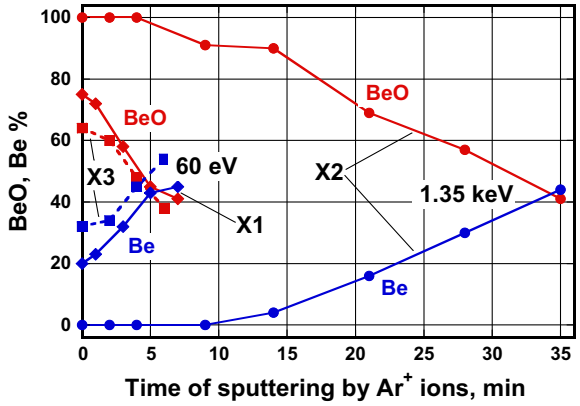

Fig. 7. XPS data for the Be mirror specimen exposed to deuterium plasma ions: ♦ – following Ar ion cleaning (X1 in Fig. 6), $E_i = 300$ eV; ● – following the decrease of reflectance due to D^+ ion bombardment, $E_i = 1350$ eV (X2 in Fig. 6); ■ – following the restoration of reflectance due to exposure to D^+ ions, $E_i = 60$ eV after the second drop of reflectance (X3 in Fig. 6).

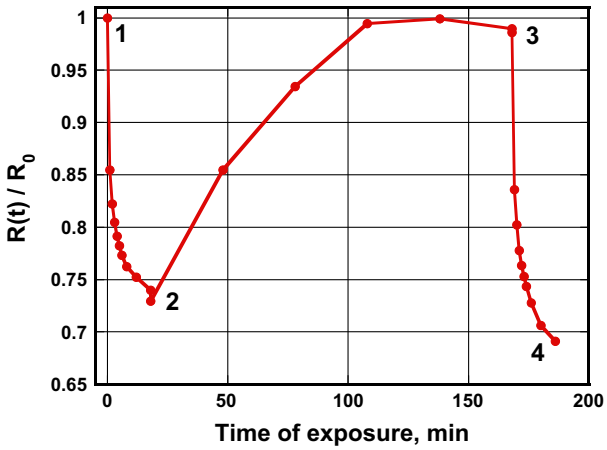

Fig. 8. Relative value of reflectance (at $\lambda = 650$ nm) as a function of the exposure time to ions from a deuterium plasma; parts 1–2 and 3–4 of the reflectance drop are a result of exposure to ions with energy 1.35 keV, the part 2–3 is the restoration of reflectance due to exposure to ions with energy 50 eV. Ion current density is 16.5 A/m^2.

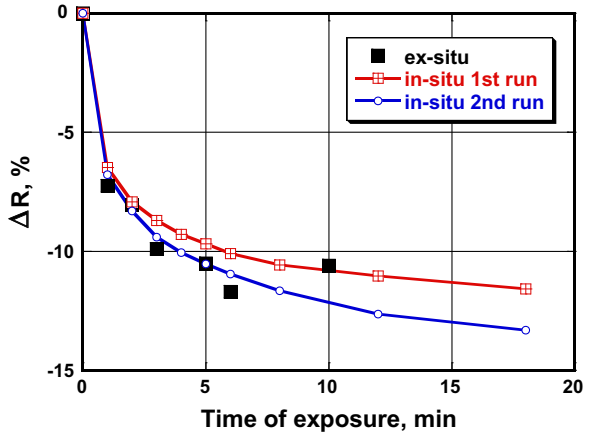

Fig. 9. Time behavior of the drop of reflectance, $\Delta R(t) = R(t) - R_0$, of Be mirror exposed to 1.35 keV deuterium plasma ions measured *in situ* and *ex situ* at $\lambda = 650$ nm. Curves with open squares and circles are, correspondingly, for the 1st run (parts 1–2 of the graph in Fig. 8) and 2nd run (parts 3–4 of the graph in Fig. 8) of the time dependence of reflectance shown in preceding figure, and the solid squares are the results of *ex situ* measurements.

3.5. Characteristics of microrelief

An attempt was made to look for a correlation between the reflectance behavior and the surface microrelief of the Be mirrors. With this aim three Be specimens (TGP-56) of similar initial structural and optical characteristics were exposed in parallel: specimen A was subjected to the cleaning procedure with 40 eV ions from the deuterium plasma; specimen B was cleaned in the same way and then bombarded with 1350 eV energy ions; and the third specimen, C, was subject to a long-term exposure of 40 eV ions following the two procedures applied to specimen B. The surfaces of all specimens were analyzed by means of an atomic field microscope (AFM) and after that the exposures to deuterium plasma ions were continued: specimen A was bombarded with 1350 eV ions, specimen B was long-term exposed to 40 eV ions, and specimen C was again bombarded with 1350 eV energy ions. Afterwards the surfaces of all three samples were analyzed a second time by AFM. The results are shown in Table 1 and Fig. 10.

It is seen that exposure of the cleaned specimen A to high energy ions (c → cd) resulted in an increase of the parameter R_q. Exposure of specimen B, after similar procedures, to low-energy ions (cd → cdr) led to an appreciable decrease of R_q. Specimen C, treated to the same exposures as B in the previous procedure, then again bombarded with high energy ions (cdr → cdrd), showed an increase of the parameter R_q. Thus, R_q increases under exposure to high energy ions and decreases when the sample is exposed to low-energy ions.

The AFM photos after the next to last and the last procedures for each specimen indicated in Table 1 are presented in Fig. 10. Measurements of spectral reflectance at times corresponding to the AFM photos are also shown; the solid lines show the reflectance before the procedure indicated under the graph and the dotted lines the reflectance after the procedure.

It is evident from a visual inspection of the photos that each time a Be mirror specimen was exposed to 1350 eV ions (procedure d), not only the roughness parameter increases as indicated in Table 1, but the spatial characteristics of the surface microroughness became more pronounced than after exposure to low-energy ions (procedures c and r). This visual impression is supported with qualitative analysis of the size distribution of spatial dimensions of surface inhomogeneities for each of Be samples, see Table 1. The analysis procedure consisted in finding a Fourier spectrum containing the harmonics associated with the longitudinal dimensions of irregularities. The sampling of relief heights was done along a spiral curve with length $L_0 = 10$ μm using the data on irregularity heights from the matrix (500 × 500 elements, 1 × 1 μm or 5 × 5 μm) representing the map of heights obtained by electronic processing of the AFM data.

Fig. 11 shows the results of such a quantitative analysis based on photos of Fig. 10; the amplitude SP for each harmonic is plotted as a function of the characteristic length, L, for that harmonic. According to these results, after procedures (c → cd) and (cdr → cdrd) were applied to specimens A and C almost all longitudinal harmonics of the spatial spectrum increased. In contrast, exposure of specimen B to low-energy ions (cd → cdr) resulted in the amplitude of practically all (mainly, medial and major) spatial harmonics decreasing.

Thus, after exposure to high or low-energy ions the harmonic contributions in the spectra of spatial inhomogeneities as well as the R_q values change in qualitative agreement with the reflectance.

Table 1
Conditions and results of exposure of samples A–C. The root mean square, R_q, i.e., the surface roughness parameter characterizing heights of irregularities and the lateral size of 'islands' along the surface, a, were calculated using the data of AFM measurements. The size of the AFM square test region is 5 × 5 μm.

Procedure; time exposures for different procedures (min)	Procedure; characteristics of surface irregularities (R_q, a) (nm)							
	Cleaning, 40 eV		Degradation-1, 1350 eV		Recovery, 40 eV		Degradation-2, 1350 eV	
	R_q	a	R_q	a	R_q	a	R_q	a
A (c140′ → cd20′)	4.0	15–25	5.4	15–55				
B (c50′ d20′ → cdr180′)			3.4	25–100	2.6	7–15		
C (c15′d20′r150′ → cdrd20′)					2.5	7–15	4.4	25–100

The abbreviations in the first column are: c – cleaning (40 eV), d – degradation (1350 eV), r – recovery (40 eV). Times of exposures are indicated in minutes.

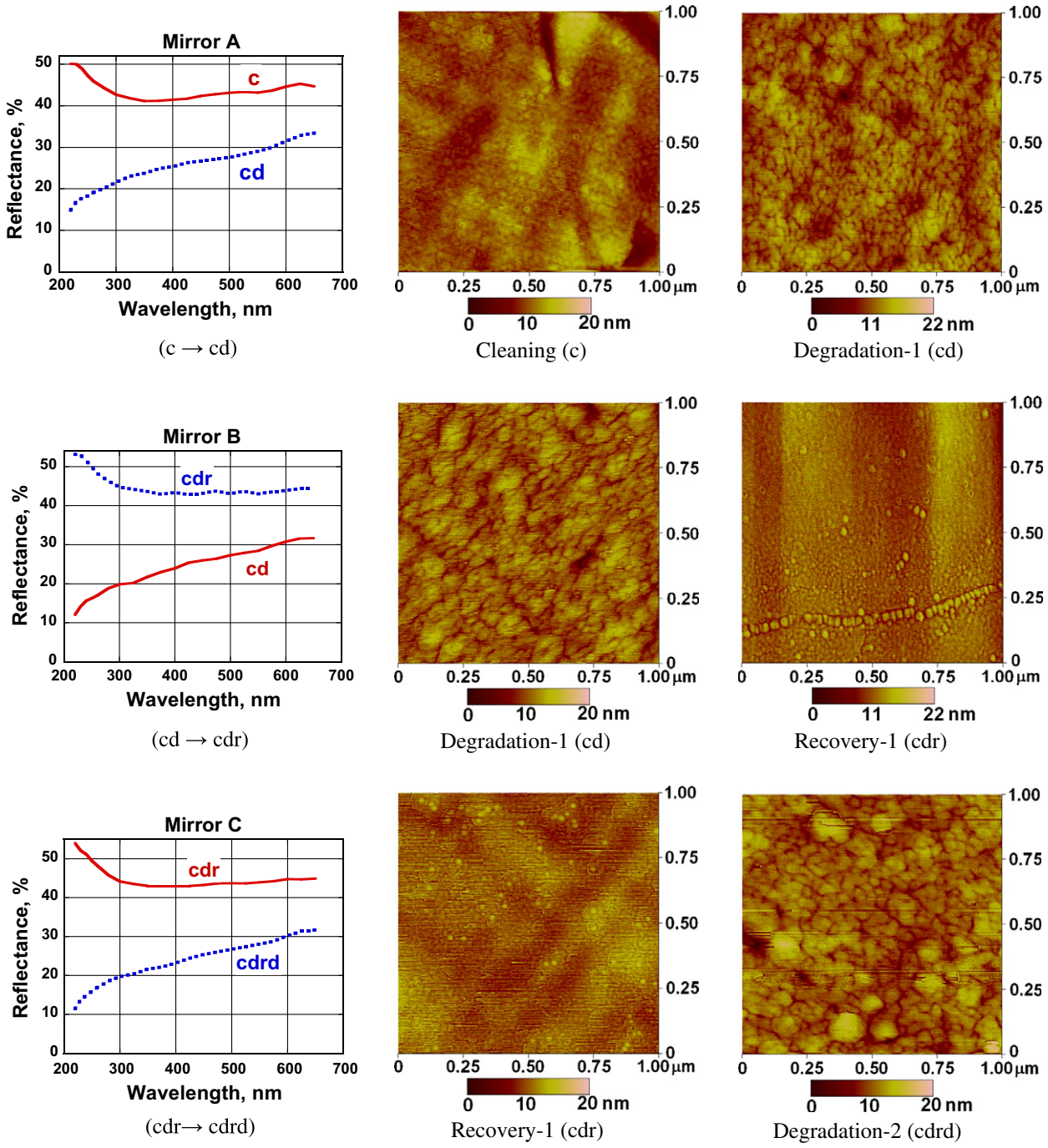

Fig. 10. AFM photos of the surface of Be mirrors after successive exposures to cleaning with low-energy ions of deuterium plasma, bombardment with 1350 eV ions, and long-term exposure to low-energy ions. A height scale is shown below every AFM micrograph.

However, it is very important to note that such modification of the surface morphology plays only a minor role in the reflectance change. Application of the Bennett formulae for specular reflectance at normal incidence as a function of surface roughness [16]:

$$R = R_0 \exp[-(4\pi d)^2/\lambda^2]$$

at $\lambda = 220$ nm and for a mean value of the surface microrelief of $d = R_q = 5$ nm gives only ~4% of the absolute reflectance decrease, in comparison to the reflectance of the smooth surface (R_0). For $\lambda = 650$ nm the decrease of reflectance is calculated to be less than 1%. Experimentally, the observed decrease in reflectance is ~30% and ~10% at these wavelengths (Figs. 6, 8 and 10). This comparison demonstrates that the observed drop of reflectance due to keV-energy ion bombardment is not connected with the development of the nm-scale irregularities seen by the AFM. However, the observed spatial irregularities probably do characterize the structure of the different surface layers, either the oxide, (e.g. specimen A state (c) or specimen B state (cdr)) or the hydroxide (e.g. specimens A and B, state (cd) or specimen C state (cdrd)).

Such a big difference between the measured reflectance changes and the ones estimated from the AFM data, indicate that the optical characteristics of the surface films (Fig. 4), and the changes to the film thickness (Figs. 5 and 7) dominate the reflectance behavior.

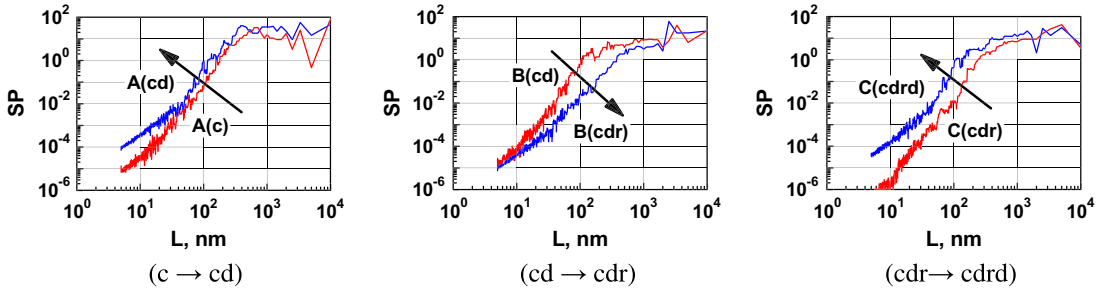

Fig. 11. The spectra of harmonics corresponding to the longitudinal size of irregularities which were obtained by means of Fourier transform along a representative length of 10 μm chosen on the surface of samples A–C. The curves were smoothed for clarity. Arrows indicate the sequence of exposures.

4. Discussion

In experiments with Al mirror samples [7], it was found that Al mirrors had very similar reflectance behavior to the Be mirror specimens. In that study, in addition to XPS, two other methods of surface analysis were applied: Auger electron spectroscopy and SIMS. The results of all these methods agreed very well [7]. As an example we show in Fig. 12 SIMS measurements of Al_3^+ clusters from three Al mirror specimens corresponding to the three surface states: "initial" – following the initial cleaning procedure with low-energy ions; "1350 eV" – after a short exposure to 1350 eV ions (subsequent to an initial cleaning); "60 eV" – following a long exposure to low-energy ions, again subsequent to the initial cleaning and the 1350 eV ion exposure. Assuming the three-atom cluster to be an indication of surface cleanliness, an increase in surface film thickness was clearly observed following the energetic ion bombardment, and a decrease following the long exposure to low-energy ions. Thus, the data of Fig. 12 are in a good agreement with the other results presented in [7].

The decrease in reflectance observed for the Be mirrors is now tied to two changes in the surface oxide layers which occur during bombardment with keV-range ions from the D^+ plasma (which includes small amounts of water vapor): (i) an increase in the thickness of the oxidized film, and (ii) modification of both optical indices, and especially important – a significant increase of extinction coefficient of the thicker films, as showed by ellipsometry (Figs. 4 and 5).

We have modeled the hydroxide film growth due to keV-ion bombardment in the following way. We start with an initial BeO film thickness of $d = 8$ nm, which begins its transformation to hydroxide just after exposure begins. As mentioned above, the minimum experimental exposure time was 1 min, and thus the minimal ion fluence to the specimen was $\sim 7 \times 10^{21}$ ion/m^2. This value is about one order of magnitude larger than the number of oxygen atoms in a BeO film of 8 nm thick, $\sim 6.2 \times 10^{20}$ O atoms/m^2 [17]. Taking into account the backward reflection of some part of the ion flux (~20% according to [18]) and the fact that a large portion of the deuterium ions contain two or three atoms [19], then it may be concluded that after 1 min of exposure, more than ten deuterium atoms are implanted into the film for every BeO molecule. The cross section for the process of oxide–hydroxide transformation under D ion implantation is not known, however, more than a factor ten difference between the fluence of D ions and the number of oxide molecules suggests that it may be reasonable to assume the near-complete transformation of the oxide into a hydroxide film according to the reaction: $2BeO + 2D \Rightarrow Be(OD)_2 + Be$. This is the first stage of the process, characterized by the full (or almost full) transformation of existing oxide film (with $k \approx 0$) into a hydroxide film (with $k > 0$) and leading to the abrupt drop in reflectance observed after 1 min exposure, Figs. 8 and 9. The second stage of the process involves the relatively slow increase in thickness of the surface layer, predominantly hydroxide, due to the continued ion bombardment. This may be due to the formation of new oxide molecules followed by a similar transformation into hydroxide and/or due to the direct creation of hydroxide molecules from the reaction of free Be atoms with water molecules. As all of the oxide molecules in the original layer are already assumed to have been converted to hydroxide, this process necessarily involves both a source of both Be and O atoms in addition to the deuterium ions, this is discussed below. It is noted that the beryllium oxide imbedded in the bulk of the specimens (along the Be grains) is unlikely to have any practical impact on the surface reactions in comparison with an impact of water vapor from the vacuum background, as there is no measurable sputtering of specimens which would be required to liberate this source of oxygen.

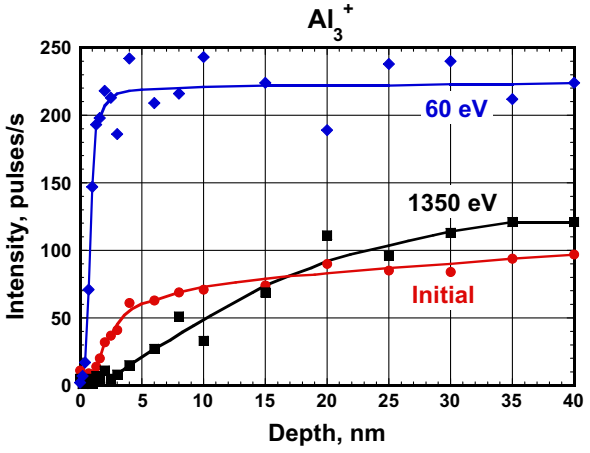

Fig. 12. Time dependence of intensity of Al_3^+ peak for three Al samples bombarded with 5 keV Ar^+ ions during SIMS measurements.

Modeling results for the hydroxide film thickness as a function of the time of exposure to keV-energy ions, based on the $\lambda = 650$ nm *in situ* reflectance data, Fig. 9a, the BeO optical indices of Fig. 4 ($n_2 = 1.74$, $k_2 = 0.05$ for Be4H) and initial thickness of BeO (8 nm) are presented in Fig. 13. Curves 1 and 2 correspond to segments 1–2 and 3–4 of the *in situ* reflectance measurement (Fig. 8) and to the curves '*in situ* 1st run' and '*in situ* 2nd run' in Fig. 9.

The time, or fluence dependence of the hydroxide layer growth, roughly from 9 nm to 16 nm in 17 min, allows us to make comparisons with the rate of oxide layer growth reported in [9]. It was found there, that approximately seven oxygen atoms were added to the layer for every 1000 incident D atoms (5 keV D_2^+ ions), or one oxygen per 140 D. In the present experiments, we assume a $Be(OD)_2$ density of ~2 g/cm^3 (instead of 1.92 g/cm^3 for $Be(OH)_2$),

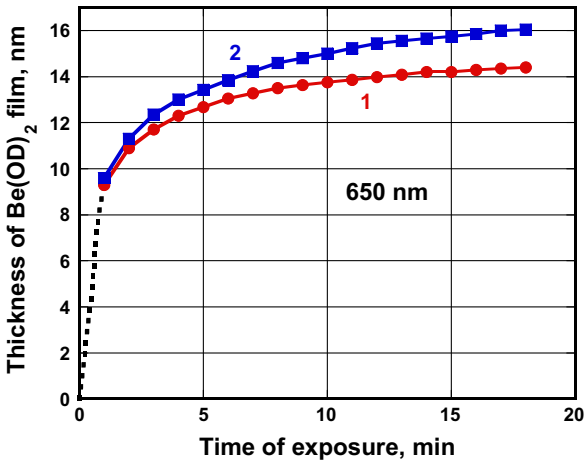

Fig. 13. Thickness of the hydroxide film calculated from the data of Fig. 9 using optical indices from the graphs in Fig. 4. Ion current density 16 A/m^2, ion energy 1.35 keV.

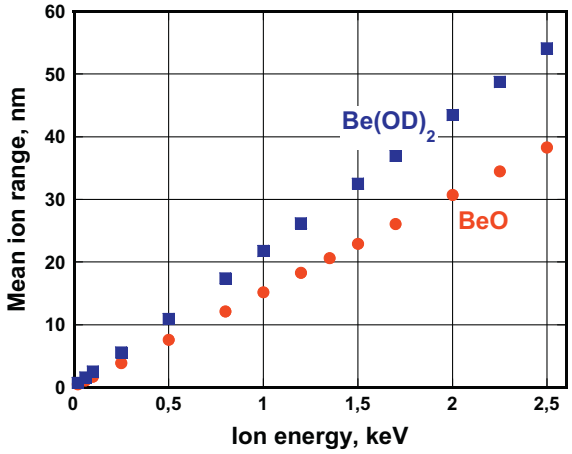

Fig. 14. The mean range of D^+ ions in BeO and $Be(OD)_2$ as a function of ion energy (SRIM, www.srim.org).

and thus the initial 9 nm thickness of hydroxide layer contains $\sim 4.8 \times 10^{20}$ O/m^2. During minutes 1–5 of the ion exposure, the film thickness increases from 9 to 13 nm, corresponding to the increase in the density of O atoms of $\sim 2.1 \times 10^{20}$ O/m^2, and experiences an ion fluence of $\sim 2.8 \times 10^{22}$ ions/m^2. Again taking into consideration particle reflection and multi-atom ions, the D atom fluence is $\sim 3.5 \times 10^{22}$ D/m^2, with the average deuterium atom energy noticeably below 1 keV. Thus, over this 4 min exposure, we add one oxygen atom for each ~170 D atoms, in reasonable agreement with [9]. As the fluence increases, this rate drops off quickly as the oxide thickness saturates while the rate remains constant in [9]. This is likely due to the lower ion energy and, hence, D atoms range in the current experiments.

One further comparison between the results of [9] and the present results is obtained from Be specimens which were bombarded with 5 keV He^+ ions and ions from the D_2 + He plasma, respectively. In [9] the rate of oxide/hydroxide growth was a factor of 13 times higher with 5 keV He^+ ions than with 2.5 keV deuterium ions. In our case, we observed an increase in the rate of reflectance degradation when Be mirror samples were exposed to 1.35 keV ions from the D_2 + He mixed plasma in comparison to ions from D_2 plasmas (Fig. 2). In both cases it appears that He^+ ions played the role of a catalyst, increasing the diffusion of Be atoms ([9]) and/or increasing the rate of breaking the bonds of BeO molecules (our experiments). The increasing rate of oxidized film growth with He ions is in some ways surprising, as, according to [20], the physical sputtering yield of BeO with 5 keV He ions is five times higher than with 2.5 keV D ions. The mechanism suggested in [9] was the radiation enhanced diffusion of beryllium atoms from the metal surface to the outer oxide film surface where they meet additional oxygen atoms and form oxide. The mechanism of beryllium atom diffusion through the oxide layer was confirmed experimentally in [21], where the kinetics of beryllium oxidation was studied as a function of temperature with the aid of two oxygen isotopes, ^{16}O and ^{18}O.

For this mechanism to be effective, the ion range in the BeO must be greater than the BeO film thickness. Range calculations (with the SRIM 2006 program) as a function of D^+ ion energy, Fig. 14, demonstrates that for our highest ion energy (1.35 eV) the mean ion range is near 20 nm, and the maximum range is about factor two longer. Thus, the mechanism of ion-induced diffusion of Be atoms through the oxide layer is consistent with the fast transformation of the initial ~8 nm thick BeO film into a hydroxide film with following much slowly increase of the transformed film thickness to a maximum of ~17 nm (ellipsometry measurements, Section 3.2 and Fig. 13).

From the AFM data (Section 3.5, Figs. 10 and 11), two further results follow. First, it should be noted that the observed scale of spatial irregularities does not correlate with the size of grains (50–60 μm, as was mentioned above). Second, the AFM data of the roughness parameter gives a measure of the quality of the mirror polishing, as the surface roughness of the bulk Be specimen cannot be not greater than the minimum roughness measured with AFM, i.e., not more than ~3 nm.

Finally we discuss the mechanism involved in the decrease of the surface layer thickness when Be (and Al) mirrors are exposed to low-energy, ~50 eV, deuterium plasma ions. The mechanism is probably a combination of both physical sputtering and chemical erosion. The importance of chemical erosion follows from the observation of reflectance restoration for ion energies as low as 20 eV [3], i.e., a little less than the threshold for the physical sputtering of BeO with D ions [20]. As the ion energy is increased to $\geqslant$40 eV, then physical sputtering becomes possible and manifests itself through the faster restoration of the reflectance for 60 eV ions in comparison with 20 eV ions [3]. If we assume the same film density as in [17], the ~17 nm thick hydroxide film will contain $\sim 9 \times 10^{20}$ O atoms/m^2. The fluence of low-energy ions can be taken from the graph for reflectance restoration shown in Fig. 8 (parts 2–3 of the curve); the value averaged over 90 min restoration procedure is $\sim 5.6 \times 10^{23}$ ion/m^2. Thus the cleaning efficiency is ~620 deuterium ions per every O atom removed from the film. Taking into account the multi-atom ions in the plasma, the efficiency is approximately 1000 D atoms per every atom of oxygen. This value is in reasonable agreement with published data for some other metals [22]: ~130 D atoms for NiO, ~300 – for Fe_2O_3 and Mo_xO_y, and ~500 D atoms for TiO_2.

5. Conclusions

The optical properties of Be and Al mirrors subjected to impact by keV-energy ions from a deuterium plasma contaminated with oxygen were found to be very sensitive to chemical processes on the specimen surface, in particular, to the conversion of a relatively thin oxide layer to a thicker hydroxide layer. AFM measurements have shown the hydroxide film to have a modulated structure with a longitudinal size in the range 20–100 nm and ~5 nm vertically. However, such surface structure has only a minor effect on the reflectance drop due to keV-energy deuterium plasma ions, which is primarily caused by the modified film having a non-zero extinction index (as distinct from the BeO film).

Ion-induced diffusion of Be atoms through the surface oxide layer is thought to be a critical part of the surface layer growth, and this is connected to the ion range in the film. Ultimately, there is a balance between physical sputtering from the oxide layer surface, and the reformation of the oxide/hydroxide layer through ion-induced diffusion. The effect appears to be stronger if helium is added to the deuterium plasma (which may be important for ITER).

The oxide–hydroxide film, can be slowly eroded by the impact of low-energy deuterium ions (20–50 eV) restoring the original optical characteristics of Be (and Al) mirrors. This is thought to be the result of a combination of chemical erosion and physical sputtering processes.

The very high sensitivity of the optical characteristics of polished Be or Al surfaces to the nature and thickness of the surface film suggests that optical methods might be used for the *in situ* control of the chemical modification of these materials, even if they are not being used as mirrors.

Acknowledgements

Part of this work, supported by Canadian Government, was carried out within the framework of the STCU Project #3668. The authors thank Prof. A.I. Belyaeva and Dr. A.A. Galuza for providing the ellipsometric measurements.

References

[1] V.G. Konovalov, A.V. Babun, V.N. Bondarenko, I.I. Papirov, I.V. Ryzhkov, A.N. Shapoval, A.F. Shtan', S.I. Solodovchenko, A.A. Vasiliev, V.S. Voitsenya, L. Jacobson, D.V. Orlinski, Plasma Dev. Oper. 10 (2002) 169–177.
[2] A.F. Bardamid, A.I. Belyayeva, V.N. Bondarenko, A.A. Galuza, V.V. Gann, L. Jacobson, V.G. Konovalov, D.V. Orlinskij, I.I. Papirov, I.V. Ryzhkov, A.N. Shapoval, A.F. Shtan', S.I. Solodovchenko, A.A. Vasil'ev, V.S. Voitsenya, J. Nucl. Mater. 313–316 (2003) 112–115.
[3] V.S. Voitsenya, A.F. Bardamid, V.N. Bondarenko, V.G. Konovalov, D.V. Orlinskij, I.V. Ryzhkov, A.N. Shapoval, A.F. Shtan', S.I. Solodovchenko, K.Yu. Vukolov, J. Nucl. Mater. 329–333 (2004) 1476–1480.
[4] G. De Temmerman, M.J. Baldwin, R.P. Doerner, D. Nishijima, R. Seraydarian, K. Schmid, F. Kost, Ch. Linsmeier, L. Marot, J. Appl. Phys. 102 (2007) 083302.
[5] J. Gardner, The James Webb Space Telescope, Proc. Sci. <http://pos.sissa.it/archive/conferences/052/005/MRU_005.pdf>, 2007.
[6] M.W. Werner, T.L. Roellig, F.J. Low, et al., The spitzer space telescope mission, Astrophys. J. Suppl. 154. <http://arxiv.org/abs/astro-ph/0406223v1>, 2004.
[7] A.F. Bardamid, A.I. Belyaeva, J.W. Davis, M.V. Dobrotvorskaya, A.A. Galuza, L.M. Kapitonchuk, V.G. Konovalov, I.V. Ryzhkov, A.F. Shtan', K.A. Slatin, S.I. Solodovchenko, V.S. Voitsenya, J. Nucl. Mater. 393 (2009) 473–480.
[8] M. Silberberg, Chemistry: The Molecular Nature of Matter and Change, McGraw-Hill, 2004 (Group 3A(13): The Boron Family, 1216p, Chapter 14.5).
[9] R.A. Langley, J. Nucl. Mater. 85 & 86 (1979) 1123–1126.
[10] V.M. Sharapov, V.Kh. Alimov, L.E. Gavrilov, J. Nucl. Mater. 258–263 (1998) 803–807.
[11] A.F. Bardamid, V.T. Gritsyna, V.G. Konovalov, D.V. Orlinskij, A.N. Shapoval, A.F. Shtan', S.I. Solodovchenko, V.S. Voitsenya, K.I. Yakimov, Surf. Coat. Technol. 103–104 (1998) 365–369.
[12] D.V. Orlinski, V.S. Voitsenya, K.Yu. Vukolov, Plasma Dev. Oper. 15 (2007) 33–75.
[13] V.G. Konovalov, M.N. Makhov, A.N. Shapoval, I.V. Ryzhkov, A.F. Shtan', S.I. Solodovchenko, V.S. Voitsenya, The method for in situ monitoring of the quality of in-vessel mirrors in a fusion reactor, Probl. Atom. Sci. Technol. #1 (59) 2009, 13–15. <http://vant.kipt.kharkov.ua/TABFRAME.html>.
[14] J.H. Weaver, D.W. Lynch, R. Rosei, Phys. Rev. B 7 (1973) 3537–3541.
[15] H. von Gruner, Einige lichtoptische Eigenschaften reaktiv aufgedampfter Berylliumoxid-Schichten, Optik 39, Heft 4 (1974), Seiten 443–449.
[16] H.E. Bennett, J. Opt. Soc. Am. 53 (1963) 1389–1393.
[17] S. Zalkind, M. Polak, N. Shamir, Phys. Rev. B 71 (2005) 125413 (7).
[18] W. Eckstein, Sputtering, Reflection and Range Values for Plasma Edge Codes, IPP 9/117, Max-Planck-Institute for Plasma Physics (March 1998).
[19] K.S. Golovanivsky, V.D. Dugar-Jhabon, V.D. Shchepilov, et al., Sov. J. Plasma Phys. 7 (1981) 324.
[20] J. Roth, J. Bohdansky, R.S. Blewer, W. Ottenberger, J. Nucl. Mater. 85 & 86 (1979) 1077–1079.
[21] J. Roth, W.R. Wampler, W. Jacob, J. Nucl. Mater. 250 (1997) 23–28.
[22] Yu. Sakamoto, Yu. Ishibe, Japn. J. Appl. Phys. 19 (1980) 839–843.